STAT3 Induction of miR-146b Forms a Feedback Loop to Inhibit the NF- B to IL-6 Signaling Axis and STAT3-Driven Cancer Phenotypes

Citation

Published Version

Permanent link

Terms of Use

Share Your Story

STAT3 Induction of MiR-146b Forms a Feedback Loop to Inhibit the NF-κB to IL-6 Signaling Axis and STAT3-Driven Cancer Phenotypes

Michael Xiang[1], **Nicolai J. Birkbak**[3], **Vida Vafaizadeh**[4], **Sarah R. Walker**[1,2], **Jennifer E. Yeh**[1], **Suhu Liu**[1], **Yasmin Kroll**[1], **Mark Boldin**[5,#], **Konstantin Taganov**[5,^], **Bernd Groner**[4], **Andrea L. Richardson**[3], and **David A. Frank**[1,2,*]

[1]Department of Medical Oncology, Dana-Farber Cancer Institute, Boston, MA 02215, USA

[2]Departments of Medicine, Brigham and Women's Hospital and Harvard Medical School, Boston, MA 02215, USA

[3]Departments of Pathology, Brigham and Women's Hospital and Harvard Medical School, Boston, MA 02215, USA

[4]Georg-Speyer-Haus, Institute for Biomedical Research, Frankfurt, Germany

[5]Division of Biology, California Institute of Technology, Pasadena, CA 91125, USA

Abstract

Interleukin-6 (IL-6)-mediated activation of signal transducer and activator of transcription 3 (STAT3) is a mechanism by which chronic inflammation can contribute to cancer and is a common oncogenic event. We discovered a pathway the loss of which is associated with persistent STAT3 activation in human cancer. We found that the gene encoding the tumor suppressor microRNA *miR-146b* is a direct STAT3 target gene and its expression was increased in normal breast epithelial cells but decreased in tumor cells. Methylation of the *miR-146b* promoter, which inhibited STAT3-mediated induction of expression, was increased in primary breast cancers. Moreover, we found that miR-146b inhibited nuclear factor κB (NF-κB)-dependent production of IL-6, subsequent STAT3 activation, and IL-6/STAT3-driven migration and invasion in breast cancer cells, thereby establishing a negative feedback loop. In addition, higher expression of *miR-146b* was positively correlated with patient survival in breast cancer subtypes with increased *IL6* expression and STAT3 phosphorylation. Our results identify an epigenetic mechanism of crosstalk between STAT3 and NF-κB relevant to constitutive STAT3 activation in malignancy and the role of inflammation in oncogenesis.

*To whom correspondence should be addressed: david_frank@dfci.harvard.edu.
#**Current address:** Department of Molecular and Cellular Biology, Beckman Research Institute, City of Hope, Duarte, CA 91010, USA
^**Current address:** EMD Millipore, 28820 Single Oak Drive, Temecula, CA 92590, USA

Introduction

Signal transducers and activators of transcription (STATs) are proteins in a family of transcription factors that have key roles in cancer. In particular, the deregulation and inappropriate activation of STAT3 plays a central role in cancer pathogenesis (*1*). In normal cells, STAT3 activation is transient and tightly controlled in extent and duration. By contrast, in many cancers, STAT3 is constitutively active, leading to continued expression of target genes that promote cell proliferation, survival, invasion, and angiogenesis. A major driver of STAT3 activation in malignancy is the cytokine interleukin-6 (IL-6) (*2*), which signals through a complex of IL-6 receptor α (IL-6Rα) and gp130 to activate Janus kinases (JAKs) and induce tyrosine phosphorylation of STAT3. The importance of IL-6-driven STAT3 activation has been demonstrated in multiple tumor types, including breast, lung, liver, prostate, pancreatic, colon, head and neck, multiple myeloma, and melanoma (*3, 4*).

The source of IL-6 can be either paracrine, originating from nearby stromal or inflammatory cells, or autocrine, produced by tumor cells (*5*). Specifically, the transcription factor NF-κB regulates the autocrine expression of IL-6 (*6*) and is a common mediator of cancer pathogenesis and development. For example, NF-κB can trigger an epigenetic switch leading to neoplastic transformation through induction of IL-6 and STAT3 activation (*7, 8*). Additionally, the signaling cascade of NF-κB, IL-6, and STAT3 promotes proliferation, survival, and chemotherapy resistance in breast cancer (*9, 10*), androgen-independent prostate cancer (*11, 12*), angiosarcoma (*13*), and colitis-associated cancer (*14, 15*). Therefore, NF-κB-dependent IL-6 production is a driver of STAT3 activation and thus STAT3-dependent cellular phenotypes.

Whereas many protein-coding target genes of STAT3 have been characterized, the microRNA (miRNA) target genes of STAT3 represent an interesting and relatively unexplored field of study. MiRNAs are short, non-coding RNAs that regulate messenger RNAs through translational inhibition and transcript degradation (*16*), and as with STAT3, have been found to influence virtually all aspects of tumor biology. The most well-established STAT3 miRNA target is miR-21, which has myriad oncogenic effects (*17*). IL-6-mediated expression of *miR-21* and *miR-181b-1* through STAT3 represses the translation of transcripts that encode phosphatase and tensin homolog (PTEN) and the deubiquitinase cylindromatosis (turban tumor syndrome) (CYLD), respectively, facilitating the activation of NF-κB and the maintenance of cellular transformation (*8*). The *miR-17/92* cluster is also a STAT3 target (*18*), and STAT3-mediated induction of *miR-17* expression in particular can confer resistance to MEK inhibitors (*19*). Lastly, in a model of hepatocellular carcinogenesis, STAT3 induces miR-24 and miR-629, which collectively repress hepatocyte nuclear factor 4α (HNF4α) and aid in sustaining constitutive IL-6-STAT3 signaling (*20*).

Given the functional importance of both STAT3 and miRNAs in cancer, the role of STAT3 as a transcription factor, and the dearth of known STAT3 miRNA targets, we focused on elucidating novel STAT3-regulated miRNAs with relevance to cancer. Here, we identified *miR-146b* as a direct STAT3 target gene whose expression is dysregulated in neoplastic tissue. Furthermore, we demonstrate the role of miR-146b in a feedback circuit involving

STAT3, NF-κB, and IL-6 with relevance to human cancer. Our findings suggest that the regulation of miR-146b by STAT3 is a tumor suppressor mechanism whose loss contributes to cancer pathogenesis, especially in the context of dual-activation of NF-κB and STAT3, as occurs in inflammatory states.

Results

Genome-wide screen for STAT3-regulated miRNAs reveals miR-146b as a STAT target

Our initial goal was to discover STAT3-regulated miRNAs that are key signaling modulators. To do so, we generated a cellular system in which STAT3C, a constitutively-active STAT3 construct (*21*), is inducibly regulated by doxycycline. Unlike kinase or cytokine-based signaling, which may also activate other pathways, this strategy enabled specific and focused activation of STAT3. We utilized non-tumorigenic MCF-10A breast epithelial cells because, unlike many tumor cell lines, these cells do not exhibit STAT3 activation at baseline, and they have been used previously to study the biological effects of STAT3 (*22*). Therefore, MCF-10A cells are well-suited for the identification of miRNAs dependent upon STAT3 activity. The engineered MCF-10A cells responded robustly to doxycycline treatment with induction of STAT3C expression and STAT3 target genes (fig. S1, A and B).

An analysis of differentially-expressed miRNAs following STAT3C induction revealed 12 species with 2-fold or greater change in expression (fig. S1C and table S1). Five of the 12 passed validation by quantitative real-time polymerase chain reaction (qRT-PCR) (Fig. 1A), including *miR-21*, a known STAT3 target (*17*). . To distinguish the direct targets of STAT3 from those regulated indirectly, we analyzed the miRNA primary transcripts for induction by IL-6-mediated STAT3 activation while new protein synthesis was blocked (fig. S1D). This revealed miR-146b as a direct STAT miRNA target.

STATs directly regulate MiR-146b at its promoter

Induction of STAT3C in MCF-10A cells demonstrates that STAT3 activity alone is sufficient to induce miR-146b; a similar result was obtained with an inducible construct of a constitutively-active STAT5 (fig. S1, E-F). Furthermore, miR-146b was induced by cytokines that activate STAT3 (IL-6) or STAT1 (IFN-γ) (Fig. 1B). Cytokine-stimulated induction of miR-146b was abrogated by dominant-negative STAT constructs (Fig. 1C), demonstrating that STAT transcriptional activity is necessary in this context. Cytokine-stimulated activation of STAT5 was not evaluated because MCF-10A cells lack abundance of the prolactin receptor (*23*)(*23*)((*23*).

We compared the regulation of miR-146b with that of miR-146a, which shares 91% sequence identity, but resides at a distinct genomic locus. *MiR-146a* is a well-characterized NF-κB target (*24*), but it is not known if NF-κB regulates miR-146b. In MCF-10A cells, STAT activation induced the abundance of miR-146b but not miR-146a, whereas NF-κB activation induced by TNF-α showed the opposite pattern (Fig. 1D). Moreover, TNF-α induced only the abundance of miR-146a and not miR-146b in immortalized mammary

epithelial cells (IMECs) (fig. S1G), together suggesting that miR-146b is a target of STAT but not NF-κB.

To elucidate how STATs regulate miR-146b at a molecular level, we first analyzed the 3kb genomic region upstream of *miR-146b*. Using 5' rapid amplification of cDNA ends (RACE), the start site for the transcript was mapped to position -741 relative to the primary transcript. Two consensus STAT binding motifs were found in islands of high phylogenetic conservation located 830 bp and 1700 bp upstream of the primary transcript (Fig. 1E). When this 3 kb region was inserted upstream of a luciferase reporter, it conferred responsiveness to cytokine treatment and STAT3C (Fig. 1F). Mutagenesis of either STAT site inhibited reporter induction, thus establishing both sites as functional. Additionally, electrophoretic mobility shift assay (EMSA; Fig. 1G) and ChIP (Fig. 1H) demonstrated direct binding of IL-6-activated STAT3 to the distal site. The high GC content around the proximal site precluded the ability to quantitate STAT binding by ChIP.

STAT activation induces miR-146b in normal tissue and non-transformed cells, but not in tumors or cancer cells

To investigate the regulation of miR-146b in normal physiology, we examined mouse mammary epithelium at various developmental stages, because STAT activation is well-characterized in this context. Prominent induction of miR-146b, but not miR-146a, occurred throughout late pregnancy, lactation, and involution (Fig. 2A), paralleling recognized patterns of STAT phosphorylation (Fig. 2A) and target gene expression (fig. S2) in the same tissue. Thus, *miR-146b* appears to be a bona fide STAT-regulated gene in vivo. In a wide range of cell lines lacking basal STAT activation (fig. S3), the induction of *miR-146b* expression after cytokine treatment was effectively partitioned between a moderate to large increased abundance in non-tumorigenic, non-transformed cell lines (derived from mammary, pancreatic, and prostate epithelium) and little to no induction in nearly all cancer cell lines (Fig. 2B). These data suggest that STAT regulation of *miR-146b* expression occurs under normal physiological conditions, but is lost in malignancy. To examine this further, we studied a panel of breast cancer cell lines with constitutively active STAT3. These cells did not have increased *miR-146b* expression relative to that seen in unstimulated, non-cancerous MCF-10A cells that lack basal STAT3 activation (Fig. 2C). Furthermore, we measured the abundance of miR-146b in a cohort of primary invasive breast cancers that had activated STAT3 (evident by the tyrosine phosphorylation of nuclear STAT3 detected by immunohistochemistry). We found that *miR-146b* expression did not increase with greater STAT3 activation, and in fact decreased (Fig. 2D). This suggests that, in vivo, tumors with increased STAT3 activation experience selective pressure to decrease *miR-146b* expression, consistent with a functional role for miR-146b as a tumor suppressor. Together, these findings indicate that miR-146b is a STAT-regulated gene under physiological conditions but not in cancer cells..

DNA methylation inhibits mir-146b expression in vitro and in vivo

To explain this loss of regulatory capacity on a target gene, we hypothesized that STAT regulation of miR-146b was disrupted in malignant cells at the epigenetic level. Given the role of DNA methylation in suppressing gene expression in tumor cells, we investigated

whether methylation inhibits STAT3 activity at the *miR-146b* promoter. To address this possibility, we first treated the miR-146b luciferase reporter with a CpG methyltransferase before transfection into MCF-10A cells. Methylation of this construct (fig. S4A) decreased its responsiveness to STAT3C by approximately 70% (Fig. 3A). Next, we examined the effect of methylation on endogenous miR-146b expression in multiple breast cancer cell lines with constitutive JAK-dependent STAT3 activation (*25*). Treatment of these cells with the demethylating agent 5-azacytidine induced the abundance of both mature miR-146b and its primary transcript (Fig. 3B). However, this induction was prevented by co-treatment with a JAK inhibitor, demonstrating that both DNA demethylation and STAT3 activity were necessary for the induction of miR-146b. Additionally, this induction pattern mirrored that of *SOCS3* (fig. S4B), which encodes a STAT3-dependent negative regulator and is frequently methylated in cancer (*1*).

To corroborate these findings in primary tumors, we utilized The Cancer Genome Atlas (TCGA). This database contains over 500 breast cancer samples with methylation of 485,000 CpGs measured at single-nucleotide resolution. Methylation at the 6 CpGs closest to *miR-146b* (within 600 bp) was significantly and inversely correlated with expression of *miR-146b* (Fig. 3C and fig. S4C) but not with another STAT3 target *miR-21* (fig. S4D). Additionally, methylation among the 6 sites was correlated with one another (fig. S4E), indicating that they are likely coordinately regulated. To evaluate methylation in this region more directly, quantitative methylation-specific PCR (Q-MSP) was performed on genomic DNA from non-transformed MCF-10A cells or from three breast cancer cell lines. Consistent with the analysis of the TCGA data, no methylation was observed in any of the cells in sites between 800 bp and 2 kb upstream of *miR-146b*. By contrast, analysis of the region including CpG sites at −63, −56, and +70 bp showed prominent methylation in all three cancer cell lines and none in the MCF-10A (Fig. 3D). Lastly, methylation of the CpG island at −56 bp from *miR-146b* was significantly higher in primary breast tumors compared with matched normal breast tissue (Fig. 3E). Thus, numerous lines of evidence show that upstream methylation suppresses *miR-146b* expression, both in cancer cell lines and in human tumors, supporting the role of miR-146b as a possible tumor suppressor.

MiR-146b counteracts the NF-κB to IL-6 (NF-κB/IL-6) signaling axis and prevents autocrine IL-6-dependent STAT3 activity

Because STAT3-dependent regulation of *miR-146b* expression was altered between normal and tumor cells, we investigated the biological relevance of miR-146b as a STAT3-responsive gene. MiR-146b targets *TRAF6* and *IRAK1* mRNA, which encode proteins that activate NF-κB (*24*). Accordingly, transfection of a miR-146b mimic repressed the translation of TRAF6 and IRAK1 in multiple breast cancer cell lines (fig. S5A). To determine whether induction of endogenous miR-146b could have the same effect, MCF-10A cells were treated with IL-6 or IFN-γ; these treatments also decreased the abundance of TRAF6 and IRAK1 (Fig. 4A), but this decrease was blunted by a miR-146b inhibitor, showing that the effect was dependent on induction of miR-146b. Thus, STAT-mediated induction of endogenous miR-146b was functionally equivalent to the effects of a miR-146b mimic.

Because IRAK1 and TRAF6 are upstream in the activation of NF-κB, we examined the effect of miR-146b on NF-κB activity in cells that have constitutively active NF-κB. Introducing a miR-146b mimic into SUM-159 or MDA-MB-468 cells decreased the expression of an NF-κB-dependent luciferase reporter gene (Fig. 4B). Similarly, introduction of the miR-146b mimic into BT-549, MDA-MB-468, or SUM-159 breast cancer cells decreased virtually all NF-κB target genes tested in each of these 3 cell lines (Fig. 4C), indicating a substantial suppression of NF-κB activity. Among the genes with decreased expression was that which encodes IL-6, which can activate STAT3 in an autocrine manner. Therefore, we hypothesized that miR-146b functions in a negative feedback loop to counter-regulate NF-κB-dependent *IL6* expression and downstream activation of STAT3. SiRNAs targeting *IL6* or the NF-κB subunit *RelA* in SUM-159 cells reduced the expression of *IL6*, the tyrosine phosphorylation of STAT3, and the expression of STAT3 target genes (Fig. 4D). STAT3 tyrosine phosphorylation was also abolished by treatment with a pharmacological inhibitor of JAK or a neutralizing antibody to IL-6 (Fig. 4E). These results underscore the role of autocrine IL-6 in the activation of STAT3. STAT3 tyrosine phosphorylation was also inhibited by miR-146b mimic, which additionally suppressed autocrine IL-6 secretion into culture medium (Fig. 4, E-F). Furthermore, miR-146b-induced inhibition of IL-6-dependent STAT3 activation was accompanied by decreased expression of a large panel of STAT3 target genes (Fig. 4G). Alternative activation of NF-κB by TNF-α, which occurs independently of TRAF6 and IRAK1, reversed all of these effects, increasing the secretion of IL-6 and the expression of NF-κB target genes (Fig. 4, E-F, and fig. S5C). These findings establish the role of miR-146b as an inhibitor of NF-κB-dependent IL-6 to STAT3 (IL-6/STAT3) signaling.

In MDA-MB-468 and BT-549 cells, the abundance and phosphorylation of STAT3 was unaffected by treatment with the IL-6 neutralizing antibody (fig. S5D), and *IL6* mRNA was substantially lower than that in SUM-159. Correspondingly, the miR-146b mimic did not inhibit the phosphorylation of STAT3 (fig. S5A). Thus, the effect of miR-146b on STAT3-related phenotypes was further characterized in SUM-159 cells.

MiR-146b inhibits IL-6/STAT3-driven migration, invasion, and the mesenchymal transition of tumor cells

Given that miR-146b inhibits autocrine IL-6-dependent STAT3 activity, we next examined its functional effects in cancer cells. Migration and invasion are promoted by STAT3 (*1*), so we hypothesized that miR-146b inhibits STAT3-dependent cancer cell motility. The introduction of miR-146b mimic into SUM-159 cells for 48 hours strongly diminished their migration and invasion (Fig. 5, A-D) without affecting cell viability as measured by cellular ATP content (fig. S6A). To determine if these effects were specifically to the result of inhibition of STAT3, STAT3C was introduced into cells to maintain STAT3 signaling independently of autocrine IL-6. STAT3C reversed the miR-146b-induced motility defects by roughly 50%, indicating that the phenotype was largely attributable to suppression of STAT3.

Cell motility is associated with epithelial-to-mesenchymal transition (EMT), a process also promoted by STAT3 (*26*). Thus, we hypothesized that miR-146b inhibits the mesenchymal

phenotype of SUM-159 cells. Indeed, miR-146b caused individual cells to become less spindle-shaped and more epithelial in appearance, whereas the overall population appeared more clustered, with increased cell-cell contacts (Fig. 5E). In addition, miR-146b caused gene expression changes that were consistent with transition to a more epithelial state (Fig. 5F). STAT3C opposed the morphological effects and some of the gene expression changes induced by miR-146b. Overall, our data show that miR-146b inhibits IL-6/STAT3-driven migration, invasion, and EMT of cancer cells.

JAK inhibition and miR-146b repletion have a combinatorial effect on tumor viability

JAK inhibitors are under investigation or in clinical use for treating malignancies that have constitutively active STAT, including those with IL-6-dependent STAT3 activation (*27*). Treating SUM-159 cells with a pharmacological JAK inhibitor for 96 hours decreased their viability (Fig. 5G). However, by shutting off STAT3, JAK inhibition also substantially reduced the expression of *miR-146b* (fig. S6B). Therefore, we hypothesized that JAK inhibition and miR-146b repletion together could exert a combinatorial effect on tumor viability. Indeed, the combination treatment had a greater effect than either agent alone (Fig. 5G), perhaps because JAK inhibition by itself decreased STAT3-dependent negative feedback regulators, such as miR-146b.

In primary breast cancers, *miR-146b* expression correlates with patient survival in molecular subtypes associated with IL-6-dependent STAT3 activation

Our data suggest that miR-146b centrally mediates a negative feedback circuit connecting STAT3 activation to decreased NF-κB activity and IL-6 production, thereby inhibiting further STAT3 activity (Fig. 6A). In breast cancer, ER negative tumors (including triple negative or basal-like tumors) are most likely to have IL-6/STAT3 signaling (20, 27). Consistent with this, SUM-159 cells are triple negative in origin. In the TCGA cohort, ER negative and triple negative tumors displayed higher *IL6* expression compared with other molecular subtypes (Fig. 6B and fig. S7A). Additionally, *IL6* expression was strongly correlated with the expression of multiple NF-κB target genes (fig. S7B), suggesting that *IL6* expression in primary tumors is also largely dependent on NF-κB.

To determine the clinical significance of miR-146b, we examined patient survival according to *miR-146b* expression within different molecular subtypes of breast cancer. Higher abundance of miR-146b, as assessed by Illumina miRNA-seq, was associated with superior overall survival specifically in the subset of patients with ER-negative tumors (Fig. 6C) or triple negative tumors (fig. S7C), which are the subtypes most linked to IL-6-dependent STAT3 activation. By contrast, there was no significant correlation of miR-146b with survival in other breast cancer subtypes, which are less likely to have STAT3 activation. This is consistent with our findings in SUM-159 cells, in which the tumor suppressor effects of miR-146b were realized largely through suppression of autocrine IL-6 and STAT3 signaling.

Discussion

STAT3 induces miR-146b, a negative regulator in cancer

Using an inducible form of constitutively active STAT3, we identified miR-146b as a STAT3 target. Although several other miRNA targets of STAT3 have been previously reported, miR-21 was the only known target to be identified in our screen. This suggests that the target genes of STAT3 are highly context-dependent, varying according to differences in epigenetic marks and chromatin structure, expression of transcriptional cofactors, or activity of other signaling pathways. We observed this phenomenon for miR-146b as well: Its regulation and expression was substantially altered (decreased) in human tumors and cancer cell lines compared to non-cancer cells and the normal developing mammary gland (Fig. 2).

In contrast to the pro-oncogenic role of nearly all other known STAT3 target genes, published studies have characterized miR-146b as a tumor suppressor. The same is true of miR-146a. Although STATs do not regulate miR-146a, it shares overlapping targets with miR-146b owing to an identical seed region. Thus, functional effects for miR-146b may be inferred from studies of miR-146a. Tumor suppressor activities for both miR-146 isoforms have been identified in breast cancer (*28, 29*), glioblastoma (*30, 31*), pancreatic cancer (*32*), gastric cancer (*33*), and androgen-independent prostate cancer (*34, 35*). These reports have identified mRNAs encoding matrix metalloproteinase MMP16, epidermal growth factor receptor (EGFR), and Rho-associated, coiled-coil containing protein kinase 1 (ROCK1) as targets of miR-146a and miR-146b. Our findings here showed that miR-146b-mediated inhibition of STAT3 activity through the NF-κB/IL-6 axis is majorly responsible for the tumor suppressor effects of miR-146b in breast cancer.

Despite these functional data, the transcriptional regulation of miR-146b has remained poorly understood. Until now, c-fos was the only transcription factor characterized to regulate miR-146b at a molecular level (*36*). That a tumor suppressor like miR-146b is regulated by STAT3 may seem surprising because STAT3 is generally regarded as mediating oncogenic effects. However, several precedents exist for other STAT3-induced negative feedback regulators. A classic example is SOCS3, which inhibits cytokine and growth factor signaling, thereby dampening STAT3 activation. Additionally, STAT3 can induce miR-125b and the miR-17/92 cluster, which can target STAT3 itself (*18, 37, 38*).

Intriguingly, the recurring pattern among these factors and miR-146b is inhibition of STAT3 activity, either directly or indirectly. Thus, STAT3-dependent negative feedback regulators may be central to the proper temporal control of STAT3 activity, which in turn is crucial to prevent normal STAT3 activation from becoming an oncogenic event. Because the dysregulation of negative regulators can shift the net effect of pathway activation toward oncogenicity, understanding the negative regulators (such as miR-146b) is crucial to fully understanding the role of STAT3 in cancer pathogenesis.

MiR-146b links STAT3 to NF-κB and IL-6 as part of a negative feedback circuit

Our study uncovered a new mechanism of inhibitory crosstalk between STAT3 and NF-κB mediated through miR-146b. Based on our model (Fig. 6A), we posit that miR-146b normally prevents unchecked STAT3 activation from taking hold in the setting of cell-

autonomous NF-κB and IL-6 signaling. However, in cancer, this negative feedback mechanism is at least partially subverted, permitting the growth and progression of tumors dependent on the NF-κB/IL-6/STAT3 pathway. Multiple lines of evidence support this model. First, STAT3 and NF-κB are frequently co-activated in tumors (*39*), and NF-κB-dependent IL-6 production is a major driver of STAT3 activation in cancer. Second, miR-146b was readily inducible in normal mammary physiology and in non-transformed cells, but not in human tumors or most cancer cell lines. Third, *miR-146b* expression was suppressed by promoter methylation, which was increased in tumor samples compared to normal tissue. Fourth, miR-146b inhibited multiple tumorigenic phenotypes in cancer cells that have activation of the NF-κB/IL-6/STAT3 pathway. Fifth, higher *miR-146b* expression was associated with longer patient survival specifically in breast cancer subtypes that exhibit increased *IL6* expression and STAT3 activation.

Although our work mostly involved models of breast cancer, the high interdependence between STAT3 and NF-κB in diverse cancer types suggests a broader role for the STAT3/miR-146b pathway as a key mechanism of tumor suppression. For example, persistent activation of NF-κB, leading to IL-6 production and STAT3 activation, has been reported to trigger neoplastic transformation in a number of cell types (*7*). Thus, STAT3 induction of miR-146b may be a general feedback inhibitor of NF-κB-triggered tumorigenesis. In other instances, STAT3 activation is the primary event and facilitates oncogenic NF-κB activation (*40, 41*). In this context, concomitant miR-146b induction may ensure NF-κB activity does not cross the oncogenic threshold. This network motif, an incoherent feed-forward loop, reduces biological noise and is especially suited to the role of miRNAs (*42*).

Additionally, the NF-κB/IL-6/STAT3 signaling cascade is crucial in multiple tumor types, with a prominent example being colitis-associated cancer (CAC) (*14, 15*). miR-146b shows increased abundance in the transition from normal tissue to dysplasia, but decreased abundance as dysplasia progresses to CAC (*43*). This suggests miR-146b is competently induced by activated STAT3 in early lesions, but becomes dysregulated during cancer progression.

MiR-146b expression displays significance to understanding human cancer

NF-κB, IL-6, and STAT3 are important to breast cancer biology (*25, 44*); thus, miR-146b and the regulatory circuit linking these factors are likely to be important in human cancer. First, *miR-146b* expression decreased with increasing abundance of phosphorylated nuclear STAT3 in tumors, indicating it may become subverted in tumors dependent on a high degree of activated STAT3. Second, a tumor suppressor role for miR-146b in primary tumors is supported by our finding of increased *miR-146b* promoter methylation in that setting. Third, *miR-146b* expression was positively associated with patient survival in tumors linked to IL-6/STAT3 signaling, which agrees with our functional studies in cell lines. Therefore, multiple lines of evidence from human tumors indicate that miR-146b functionally interacts with STAT3 in a clinically important manner.

Although reliable delivery of miR-146b to tumors is not yet clinically feasible, alternate strategies to achieve a similar goal include expression of endogenous miR-146b using demethylating agents or developing small molecules to target the key, potentially druggable

targets of miR-146b, such as IRAK1. Eventually, therapies that inhibit JAK/STAT signaling and reconstitute miR-146b activity may be combined to enhance clinical benefit, particularly for triple-negative breast cancers, which have relatively poor prognosis and limited treatment options.

Although inflammation can promote cancer (*45*), specific genetic and epigenetic perturbations are required for it to switch from being benign to oncogenic. Cancer is still a relatively rare outcome of inflammation because of the activity of normal regulatory mechanisms. Our study elucidates one such negative feedback circuit involving STAT3, miR-146b, NF-κB, and IL-6 with significance to human cancer, thus adding to our understanding of how inflammatory networks are regulated in normal and neoplastic tissue.

Materials and Methods

High-throughput microRNA screen

Doxycycline-inducible MCF-10A cells were generated by retroviral transduction with pRevTet-On and pRevTRE (Clontech) containing STAT3C-FLAG or STAT5a1*6-FLAG as the insert. Cells were untreated or doxycycline-treated (2 μg/ml) in triplicate for 48 hours prior to RNA processing using the miRNeasy Mini Kit (Qiagen). The time point was chosen due to the kinetics of STAT3C induction, observation of increased miR-21 abundance, and previous reports of miRNA maturation requiring 12-24 hours (*17*). The screen was performed at the Molecular Diagnostics Laboratory of Dana-Farber Cancer Institute using a TaqMan qRT-PCR-based platform covering approximately 700 miRNAs.

Cell lines and tissue culture

MCF-10A cells were obtained from ATCC and cultured as previously described (*46*). RWPE-1 cells were obtained from ATCC and cultured in Keratinocyte Serum-Free Medium (Invitrogen). BT-474 cells were obtained from ATCC and cultured in RPMI-1640 + 10% FBS. Immortalized mammary epithelial cells (IMEC; from Myles Brown, DFCI) were cultured as previously described (*47*). Immortalized human pancreatic duct epithelial cells (HPDE; from Ming Tsao) were cultured as previously described (*48*). SUM-159 cells (from Kornelia Polyak, DFCI) were grown in a 1:1 mix of DMEM/F12 + 10% FBS and Mammary Epithelial Cell Growth Medium (Lonza). T-47D, SKBR3, MCF7, MDA-MB-468, BT-549, and RPMI-8226 cells were obtained and cultured as previously reported (*49-51*). The cell lines 8988S (from Ronald De Pinho, MD Anderson Cancer Center), ZR-75 (from Lindsay Harris, Yale), A431 (from Martin Hemler, DFCI), and HeLa (from Ronny Drapkin, DFCI) were grown in DMEM + 10% FBS. The cell lines MDA-MB-453 (from Lindsay Harris), MM.1S (from Kenneth Anderson, DFCI), A375 (from James Mier, Beth Israel-Deaconess medical Center, Boston, MA), A549 (from Pasi Janne, DFCI), Kelly (from Rani George, DFCI), and ME-180 (from Miriam Barshak) were grown in RPMI-1640 + 10% FBS. HT-29 cells (from David Pellman, DFCI) were grown in McCoy's 5A + 10% FBS. All cells were maintained in a humidified incubator at 37°C with 5% CO_2.

Gene expression analysis

Total RNA, including miRNAs, was harvested using the RNeasy Plus Mini Kit (Qiagen) with a modified protocol supplied by the manufacturer (below). For mRNA analysis, RNA was reverse transcribed using random hexamers and assayed by qRT-PCR as previously described (*52*). For miRNA analysis, RNA was reverse transcribed with the TaqMan reverse transcription kit, followed by qRT-PCR with TaqMan miRNA assays (Life Technologies). Primer sequences are given in table S2. Gene expression was analyzed in triplicate as mean ± SEM, normalized to 18S rRNA or beta actin (mRNA) or U6 snRNA (miRNA) .

Total RNA isolation

Cell pellets were lysed in 270 µl RLT Plus buffer + 1% β-mercaptoethanol and processed by QIAshredder and genomic DNA eliminator spin columns. The flow-through was mixed with 460µl 95% ethanol by pipetting up and down, and then run through an RNeasy spin column. The spin column was washed twice with 500 µl RPE buffer (after ethanol addition), spun once again to remove residual ethanol, and then eluted with 50 µl RNase-free H_2O. All spin steps were performed on a benchtop microcentrifuge at room temperature and 14,000 RPM for 1 min.

Western blotting and antibodies

Western blotting was performed as previously described (*53*). Antibodies to phospho-MAPK (9101), total MAPK (9102), phospho- Tyr[705] STAT3 (9131), phospho-Thr[308] Akt (9275), phospho-Ser[473] Akt (9271), total Akt (9272), TRAF6 (4743), and IRAK1 (4504) were from Cell Signaling Technology. Phospho-STAT1 (33-3400) antibody was from Invitrogen. C-terminal STAT3 antibody (sc-482), N-terminal STAT3 antibody (sc-7179), and total STAT1 antibody (sc-346) were from Santa Cruz Biotechnology. Antibody to phospho-Ser[727] STAT3 was described previously (*54*). Anti-FLAG (F1804), tubulin (T5168), and beta actin antibody (A5316) were from Sigma. All antibodies were used at 1:10000 dilution for Western blot, except for phospho-Akt antibodies, which were used at 1:2000. For use in EMSA, 2 µl antibody was pre-incubated with 2 µl nuclear extract on ice for 30 min prior to addition of binding buffer and probe. IL-6 neutralizing antibody (AB-206-NA) was from R&D Systems and used at 3 µg/ml.

RACE

To determine the transcriptional start site for miR-146b, 5' - RACE was performed using the SMART RACE cDNA amplification kit (CLONTECH) according to the manufacturer's instructions.

Luciferase assays

STAT3-responsive m67 and constitutive Renilla luciferase constructs were described previously (*55*). The miR-146b promoter luciferase was created by cloning the 3kb region upstream of miR-146b into pGL3 (Promega) using PCR primers: 5'-ATGTTAACGCGTCAGGCTGGTCTCTTAGGTACTG-3' and 5'-TGGCTCCTCGAGCAAAGTTCTTTCAGCCTGGAC-3'. To introduce TT→AA point mutations at one or both STAT binding sites, the QuikChange Lightning Site-Directed

Mutagenesis Kit (Agilent) was used. Dual-luciferase assays were performed as previously described (52) and are analyzed as mean ± SD.

Q-MSP

Genomic DNA (gDNA) was isolated from cultured cell lines using a Blood and Cell Culture DNA kit (Qiagen, Inc.) and stored at −20°C before use. 0.5 µg gDNA was used for bisulfite treatment with the EZDNA Methylation Kit (Zymo Research) according to the supplier's protocol. Methylation of the CpG sites was determined through bisulfite modification of gDNA (56) and analyzed by Q-MSP (57). MYOD1 served as internal reference. The primer sequences to amplify bisulfite converted CpG sites were designed utilizing MethPrimers software (www.ucsf.edu/urogene/methprimer). The miR-146b MSP forward primer was 5'-TTTATTTATTTTGGGAACGGGAGAC-3', and the reverse primer was 5'-GACCTTAACATTAATATTATAACACTACCG-3'. PCR reactions were carried out at 95°C for 10 min, followed by 40 cycles of 95°C for 15 s and 60°C for 60 s. PCR reaction was carried out in a 25 µl volume containing 2× SYBR Green PCR master mix (Applied Biosystems), 200 nM each primer and 10ng bisulfite-modified genome DNA. Bisulfide-converted, universally methylated human gDNA (Chemicon) served as a positive control. MYOD1 serves as internal reference. Data are mean fold change ± standard deviation of three replicates.

Transfection

Plasmid transfection was performed using Fugene HD (Promega). To introduce miRNAs (25 nM) or siRNAs (10 nM), cells were reverse-transfected using Lipofectamine RNAiMAX (Invitrogen); culture media was changed 24 hours later. Thermo Scientific Dharmacon was the source of miR-146b mimic (C-300754-03-0005), control mimic (CN-002000-01-05), miR-146b inhibitor (IH-300754-05-0005), and control inhibitor (IN-002005-01-05). Control siRNA (D-001210-03) was from Thermo Scientific Dharmacon, RelA siRNA (6261) was from Cell Signaling Technology, and IL-6 siRNA (sc-39627) was from Santa Cruz Biotechnology.

EMSA

The LightShift EMSA Kit (Pierce) was used according to the manufacturer's protocol. STAT binding reactions were performed as previously described (58) using 5'-biotinylated 25 bp probes. The primer sequences were: wild-type, 5'-ACCCTCCATTCCCGGAACTTTCAAG-3', 5'-CTTGAAAGTTCCGGGAATGGAGGGT-3'; mutant, 5'-ACCCTCCAAACCCGGAACTTTCAAG-3', 5'-CTTGAAAGTTCCGGGTTTGGAGGGT-3'. The Region B probe from the *BCL6* gene, known to bind STAT3 (53), was used as a control.

Chromatin immunoprecipitation (ChIP)

MCF10A cells were stimulated with 20 ng/ml IL-6 for 15 min. ChIP was performed essentially as described (59). Cells were sonicated using a Qsonica sonicator. Lysates were immunoprecipitated overnight with a phospho-STAT3 antibody (9131, Cell Signaling

Technologies). ChIP product was analyzed for binding to the 1.7 site using the primers (AGAGACCAGCCATCCCTTTC and TCAGGGCAGCTCTACTGAGG) by qPCR.

Migration, invasion, and viability assays

For motility assays, 10,000 cells per 24-well were transfected with miRNA or control mimic. After 48 hours, cells were detached using trypsin, spun down with trypsin neutralizing solution (Lonza), and transferred to the apical chamber in pre-warmed DMEM/F12 without additives. Pre-warmed complete SUM-159 media was added to the basolateral chamber. Cells were allowed to migrate for 8 hours through polycarbonate transwell inserts (Corning) or invade for 24 hours through growth factor-reduced Matrigel-coated inserts (BD BioCoat). The inserts were then fixed and stained in 0.5% crystal violet + 6% glutaraldehyde for 30 min, rinsed in ddH$_2$O, and swabbed with pre-wet cotton tips to remove cells from the apical surface of the membrane. Migrated or invaded cells were counted in triplicate 1 mm^2 areas and shown as mean ± SD. Cell Titer Glo (Promega) was used to measure cell viability based on cellular ATP concentration.

Enzyme-linked immunosorbent assay (ELISA)

SUM-159 cells were transfected in 6-well plates with control mimic or miR-146b mimic for 48 hours. Afterward, the media was replaced with 1mL fresh media for 9 hours and harvested. Measurement of IL-6 concentration in the conditioned medium was performed using the Human IL-6 Quantikine ELISA Kit (R&D) according to the manufacturer's instructions.

Drug treatments

5-azacytidine (Sigma) was used at 1 μM for 4 days (SUM-159) or 8 days (MDA-MB-468, BT-549). JAK inhibitor 1 (Calbiochem) was used at 1μM, unless indicated otherwise. For epigenetic studies, the drugs were refreshed with new media every 2 days. U0126 (10 μM) and LY294002 (20 μM) were from Cell Signaling Technology. All drugs were dissolved in DMSO; final DMSO volume in cell culture was 0.1-0.2%.

Computational analyses

Level 3 miRNA expression (Illumina miRNA-Seq) and mRNA expression (Agilent 244k array), level 2 DNA methylation (Illumina 450k array), and clinical parameters (patient survival and ER, PR, HER2 status) were downloaded from The Cancer Genome Atlas (TCGA) for the breast cancer data set on September 30, 2012. Pearson correlation, rank-sum test, and log-rank test were used for statistical analyses.

Primary breast tumor analysis

Phospho-STAT3 (Tyr[705]) immunohistochemistry and pathologist scoring of nuclear phospho-STAT3 staining in tumor cells were performed as previously described (*55*). Samples underwent miRNA expression profiling using the Nanostring nCounter system, followed by log2 transformation and quantile normalization. Statistical analysis was by rank-sum test and Pearson correlation.

Supplementary Material

Refer to Web version on PubMed Central for supplementary material.

Acknowledgments

References and Notes

1. Frank DA. STAT3 as a central mediator of neoplastic cellular transformation. Cancer Lett. Jun 28.2007 251:199. [PubMed: 17129668]

2. Sansone P, Bromberg J. Targeting the interleukin-6/Jak/stat pathway in human malignancies. Journal of clinical oncology : official journal of the American Society of Clinical Oncology. Mar 20.2012 30:1005. [PubMed: 22355058]

3. Hedvat M, et al. The JAK2 inhibitor AZD1480 potently blocks Stat3 signaling and oncogenesis in solid tumors. Cancer cell. Dec 8.2009 16:487. [PubMed: 19962667]

4. Hodge DR, Hurt EM, Farrar WL. The role of IL-6 and STAT3 in inflammation and cancer. Eur J Cancer. Nov.2005 41:2502. [PubMed: 16199153]

5. Grivennikov S, Karin M. Autocrine IL-6 signaling: a key event in tumorigenesis? Cancer cell. Jan. 2008 13:7. [PubMed: 18167335]

6. Libermann TA, Baltimore D. Activation of interleukin-6 gene expression through the NF-kappa B transcription factor. Molecular and cellular biology. May.1990 10:2327. [PubMed: 2183031]

7. Iliopoulos D, Hirsch HA, Struhl K. An epigenetic switch involving NF-kappaB, Lin28, Let-7 MicroRNA, and IL6 links inflammation to cell transformation. Cell. Nov 13.2009 139:693. [PubMed: 19878981]

8. Iliopoulos D, Jaeger SA, Hirsch HA, Bulyk ML, Struhl K. STAT3 activation of miR-21 and miR-181b-1 via PTEN and CYLD are part of the epigenetic switch linking inflammation to cancer. Molecular cell. Aug 27.2010 39:493. [PubMed: 20797623]

9. Ndlovu MN, et al. Hyperactivated NF-(60)B and AP-1 transcription factors promote highly accessible chromatin and constitutive transcription across the interleukin-6 gene promoter in metastatic breast cancer cells. Molecular and cellular biology. Oct.2009 29:5488. [PubMed: 19687301]

10. Matsumoto G, et al. Targeting of nuclear factor kappaB Pathways by dehydroxymethylepoxyquinomicin, a novel inhibitor of breast carcinomas: antitumor and antiangiogenic potential in vivo. Clinical cancer research : an official journal of the American Association for Cancer Research. Feb 1.2005 11:1287. [PubMed: 15709200]

11. Xiao W, et al. Co-operative functions between nuclear factors NFkappaB and CCAT/enhancer-binding protein-beta (C/EBP-beta) regulate the IL-6 promoter in autocrine human prostate cancer cells. The Prostate. Dec 1.2004 61:354. [PubMed: 15389813]

12. Domingo-Domenech J, et al. Interleukin 6, a nuclear factor-kappaB target, predicts resistance to docetaxel in hormone-independent prostate cancer and nuclear factor-kappaB inhibition by PS-1145 enhances docetaxel antitumor activity. Clinical cancer research : an official journal of the American Association for Cancer Research. Sep 15.2006 12:5578. [PubMed: 17000695]

13. Yang J, et al. Ikk4a/Arf inactivation with activation of the NF-kappaB/IL-6 pathway is sufficient to drive the development and growth of angiosarcoma. Cancer research. Sep 15.2012 72:4682. [PubMed: 22836752]

14. Grivennikov S, et al. IL-6 and Stat3 are required for survival of intestinal epithelial cells and development of colitis-associated cancer. Cancer cell. Feb 3.2009 15:103. [PubMed: 19185845]

15. Liang J, et al. Sphingosine-1-Phosphate Links Persistent STAT3 Activation, Chronic Intestinal Inflammation, and Development of Colitis-Associated Cancer. Cancer cell. Dec 22.2012

16. Bartel DP. MicroRNAs: target recognition and regulatory functions. Cell. Jan 23.2009 136:215. [PubMed: 19167326]

17. Loffler D, et al. Interleukin-6 dependent survival of multiple myeloma cells involves the Stat3-mediated induction of microRNA-21 through a highly conserved enhancer. Blood. Aug 15.2007 110:1330. [PubMed: 17496199]

18. Brock M, et al. Interleukin-6 modulates the expression of the bone morphogenic protein receptor type II through a novel STAT3-microRNA cluster 17/92 pathway. Circulation research. May 22.2009 104:1184. [PubMed: 19390056]

19. Dai B, et al. STAT3 mediates resistance to MEK inhibitor through microRNA miR-17. Cancer research. May 15.2011 71:3658. [PubMed: 21444672]

20. Hatziapostolou M, et al. An HNF4alpha-miRNA inflammatory feedback circuit regulates hepatocellular oncogenesis. Cell. Dec 9.2011 147:1233. [PubMed: 22153071]

21. Bromberg JF, et al. Stat3 as an oncogene. Cell. Aug 6.1999 98:295. [PubMed: 10458605]

22. Dechow TN, et al. Requirement of matrix metalloproteinase-9 for the transformation of human mammary epithelial cells by Stat3-C. Proceedings of the National Academy of Sciences of the United States of America. Jul 20.2004 101:10602. [PubMed: 15249664]

23. Neilson LM, et al. Coactivation of janus tyrosine kinase (Jak)1 positively modulates prolactin-Jak2 signaling in breast cancer: recruitment of ERK and signal transducer and activator of transcription (Stat)3 and enhancement of Akt and Stat5a/b pathways. Mol Endocrinol. Sep.2007 21:2218. [PubMed: 17550976]

24. Taganov KD, Boldin MP, Chang KJ, Baltimore D. NF-kappaB-dependent induction of microRNA miR-146, an inhibitor targeted to signaling proteins of innate immune responses. Proceedings of the National Academy of Sciences of the United States of America. Aug 15.2006 103:12481. [PubMed: 16885212]

25. Marotta LL, et al. The JAK2/STAT3 signaling pathway is required for growth of CD44(+)CD24(-) stem cell-like breast cancer cells in human tumors. The Journal of clinical investigation. Jul.2011 121:2723. [PubMed: 21633165]

26. Xiong H, et al. Roles of STAT3 and ZEB1 proteins in E-cadherin down-regulation and human colorectal cancer epithelial-mesenchymal transition. The Journal of biological chemistry. Feb 17.2012 287:5819. [PubMed: 22205702]

27. Kontzias A, Kotlyar A, Laurence A, Changelian P, O'Shea JJ. Jakinibs: a new class of kinase inhibitors in cancer and autoimmune disease. Current opinion in pharmacology. Aug.2012 12:464. [PubMed: 22819198]

28. Bhaumik D, et al. Expression of microRNA-146 suppresses NF-kappaB activity with reduction of metastatic potential in breast cancer cells. Oncogene. Sep 18.2008 27:5643. [PubMed: 18504431]

29. Hurst DR, et al. Breast cancer metastasis suppressor 1 up-regulates miR-146, which suppresses breast cancer metastasis. Cancer research. Feb 15.2009 69:1279. [PubMed: 19190326]

30. Katakowski M, et al. MiR-146b-5p suppresses EGFR expression and reduces in vitro migration and invasion of glioma. Cancer investigation. Dec.2010 28:1024. [PubMed: 20874002]

31. Xia H, et al. microRNA-146b inhibits glioma cell migration and invasion by targeting MMPs. Brain research. May 7.2009 1269:158. [PubMed: 19265686]

32. Li Y, et al. miR-146a suppresses invasion of pancreatic cancer cells. Cancer research. Feb 15.2010 70:1486. [PubMed: 20124483]

33. Hou Z, Xie L, Yu L, Qian X, Liu B. MicroRNA-146a is down-regulated in gastric cancer and regulates cell proliferation and apoptosis. Med Oncol. Jun.2012 29:886. [PubMed: 21347720]

34. Xu B, et al. MiR-146a suppresses tumor growth and progression by targeting EGFR pathway and in a p-ERK-dependent manner in castration-resistant prostate cancer. The Prostate. Aug 1.2012 72:1171. [PubMed: 22161865]

35. Lin SL, Chiang A, Chang D, Ying SY. Loss of mir-146a function in hormone-refractory prostate cancer. RNA. Mar.2008 14:417. [PubMed: 18174313]

36. Shao M, et al. PDGF induced microRNA alterations in cancer cells. Nucleic acids research. May. 2011 39:4035. [PubMed: 21266476]

37. Liu LH, et al. miR-125b suppresses the proliferation and migration of osteosarcoma cells through down-regulation of STAT3. Biochemical and biophysical research communications. Dec 9.2011 416:31. [PubMed: 22093834]

38. Zhang M, et al. Both miR-17-5p and miR-20a alleviate suppressive potential of myeloid- derived suppressor cells by modulating STAT3 expression. J Immunol. Apr 15.2011 186:4716. [PubMed: 21383238]

39. Lee H, et al. Persistently activated Stat3 maintains constitutive NF-kappaB activity in tumors. Cancer Cell. Apr 7.2009 15:283. [PubMed: 19345327]

40. Rokavec M, Wu W, Luo JL. IL6-mediated suppression of miR-200c directs constitutive activation of inflammatory signaling circuit driving transformation and tumorigenesis. Molecular cell. Mar 30.2012 45:777. [PubMed: 22364742]

41. Tye H, et al. STAT3-Driven Upregulation of TLR2 Promotes Gastric Tumorigenesis Independent of Tumor Inflammation. Cancer cell. Oct 16.2012 22:466. [PubMed: 23079657]

42. Ebert MS, Sharp PA. Roles for microRNAs in conferring robustness to biological processes. Cell. Apr 27.2012 149:515. [PubMed: 22541426]

43. Kanaan Z, et al. Differential microRNA expression tracks neoplastic progression in inflammatory bowel disease-associated colorectal cancer. Human mutation. Mar.2012 33:551. [PubMed: 22241525]

44. Liu M, et al. The canonical NF-kappaB pathway governs mammary tumorigenesis in transgenic mice and tumor stem cell expansion. Cancer research. Dec 15.2010 70:10464. [PubMed: 21159656]

45. Grivennikov SI, Greten FR, Karin M. Immunity, inflammation, and cancer. Cell. Mar 19.2010 140:883. [PubMed: 20303878]

46. Debnath J, Muthuswamy SK, Brugge JS. Morphogenesis and oncogenesis of MCF-10 A mammary epithelial acini grown in three-dimensional basement membrane cultures. Methods. Jul.2003 30:256. [PubMed: 12798140]

47. DiRenzo J, et al. Growth factor requirements and basal phenotype of an immortalized mammary epithelial cell line. Cancer research. Jan 1.2002 62:89. [PubMed: 11782364]

48. Ouyang H, et al. Immortal human pancreatic duct epithelial cell lines with near normal genotype and phenotype. The American journal of pathology. Nov.2000 157:1623. [PubMed: 11073822]

49. Nelson EA, et al. Nifuroxazide inhibits survival of multiple myeloma cells by directly inhibiting STAT3. Blood. Dec 15.2008 112:5095. [PubMed: 18824601]

50. Walker SR, Chaudhury M, Nelson EA, Frank DA. Microtubule-targeted chemotherapeutic agents inhibit signal transducer and activator of transcriion 3 (STAT3) signaling. Mol Pharmacol. Nov. 2010 78:903. [PubMed: 20693278]

51. Walker SR, et al. Reciprocal effects of STAT5 and STAT3 in breast cancer. Mol Cancer Res. Jun. 2009 7:966. [PubMed: 19491198]

52. Walker SR, Nelson EA, Frank DA. STAT5 represses BCL6 expression by binding to a regulatory region frequently mutated in lymphomas. Oncogene. Jan 11.2007 26:224. [PubMed: 16819511]

53. Battle TE, Arbiser J, Frank DA. The natural product honokiol induces caspase-dependent apoptosis in B-cell chronic lymphocytic leukemia (B-CLL) cells. Blood. Jul 15.2005 106:690. [PubMed: 15802533]

54. Frank DA, Mahajan S, Ritz J. B lymphocytes from patients with chronic lymphocytic leukemia contain signal transducer and activator of transcription (STAT) 1 and STAT3 constitutively phosphorylated on serine residues. J Clin Invest. Dec 15.1997 100:3140. [PubMed: 9399961]

55. Alvarez JV, et al. Identification of a genetic signature of activated signal transducer and activator of transcription 3 in human tumors. Cancer Res. Jun 15.2005 65:5054. [PubMed: 15958548]

56. Susan JC, Harrison J, Paul CL, Frommer M. High sensitivity mapping of methylated cytosines. Nucleic acids research. 1994; 22:2990. [PubMed: 8065911]

57. Herman JG, Graff JR, Myöhänen S, Nelkin BD, Baylin SB. Methylation-specific PCR: a novel PCR assay for methylation status of CpG islands. Proceedings of the National Academy of Sciences. 1996; 93:9821.

58. Battle TE, Frank DA. STAT1 mediates differentiation of chronic lymphocytic leukemia cells in response to Bryostatin 1. Blood. Oct 15.2003 102:3016. [PubMed: 12855573]

59. Walker SR, et al. STAT5 Outcompetes STAT3 To Regulate the Expression of the Oncogenic Transcriptional Modulator BCL6. Molecular and Cellular Biology. Aug 1.2013 33:2879. 2013. [PubMed: 23716595]

60. Akashi H, Han HJ, Iizaka M, Nakamura Y. Growth-suppressive effect of non-steroidal anti-inflammatory drugs on 11 colon-cancer cell lines and fluorescence differential display of genes whose expression is influenced by sulindac. Int J Cancer. Dec 15.2000 88:873. [PubMed: 11093808]
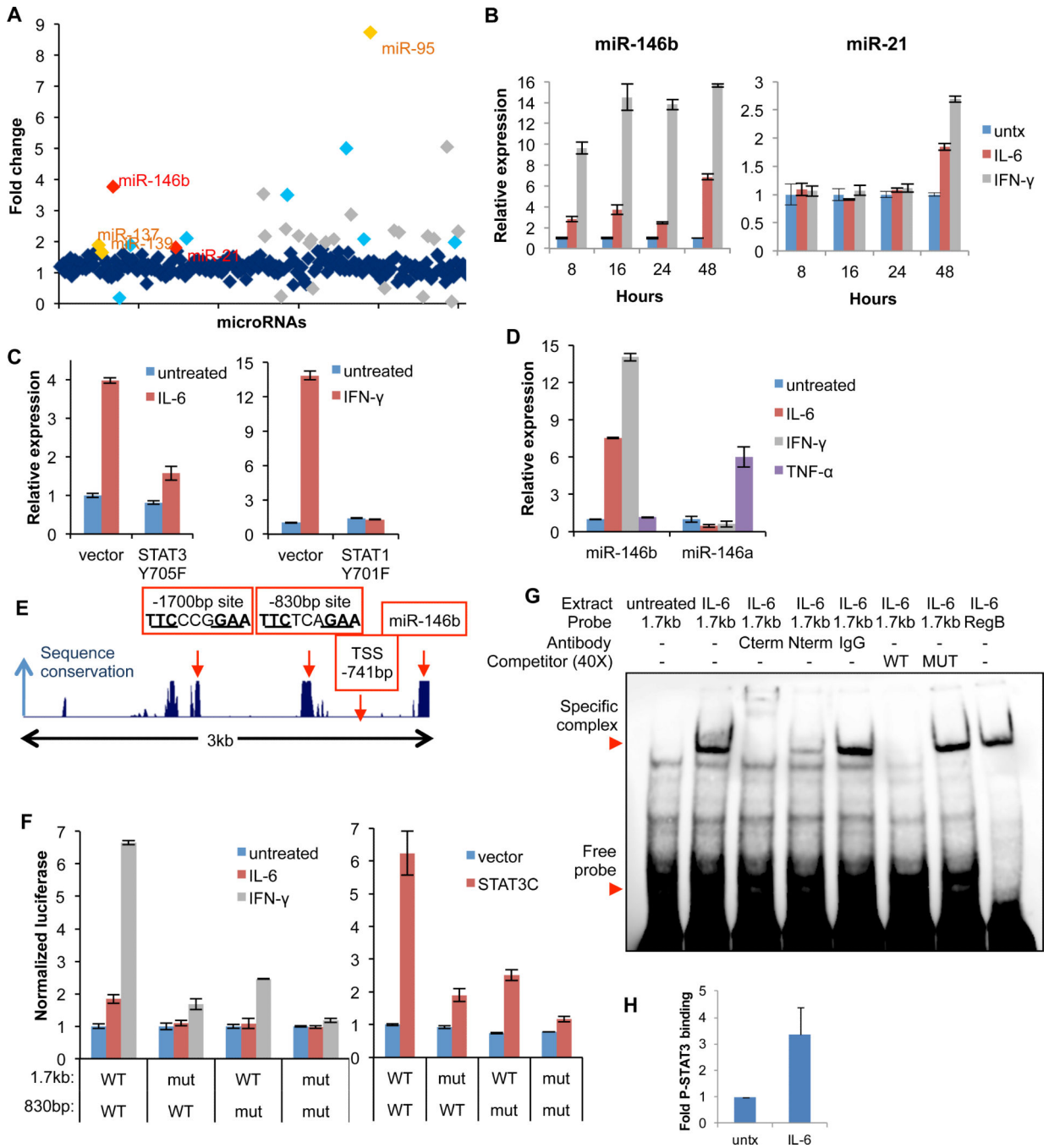
Fig. 1. STAT family members directly regulate miR-146b expression

(**A**) Genome-wide screen for STAT3-dependent miRNAs. Red and orange: direct and indirect STAT targets, respectively; light blue: hits that did not pass validation by qRT-PCR; gray: low-confidence targets not evaluated by qRT-PCR due to high screen Ct value (> 30) or lack of statistical significance. Data are fold-changes from three biological replicates. (**B**) MiRNA expression in MCF-10A cells treated with IL-6 or IFN-γ (20 ng/ml) relative to untreated (untx) cells. (**C**) MiR-146b expression in cytokine-treated (48 hours) MCF-10A cells transfected with empty vector or a dominant-negative STAT construct relative to

untreated controls. **(D)** miRNA expression in cytokine-treated (48 hours) MCF-10A cells relative to untreated controls. In (B) to (D), data are representative means ± SE from one of 2 experiments. **(E)** Schematic of the *miR-146b* promoter region (3 kb upstream) with consensus STAT binding motifs defined as TTCNNNGAA. TSS, transcription start site. **(F)** Activity of luciferase reporters containing wild-type (WT) or STAT site(s)-mutant (MUT: TT→AA) *miR-146b* promoter in shown in (E) 6 hours after cytokine treatment in wild-type MCF-10A (left) or 24 hours after STAT3C transfection in MCF-10A (right). Data are means ± SD of two independent experiments. **(G)** EMSA using nuclear extract from IL-6-treated (20 ng/ml, 15 min) MCF-10A cells and a probe centered on the 1.7 kb STAT site. Reg B: positive control. **(H)** ChIP for phosphorylated STAT3 bound to the 1.7 kb STAT site in unstimulated or IL-6-treated MCF-10A cells. Data are mean ± SD of at least two independent experiments.
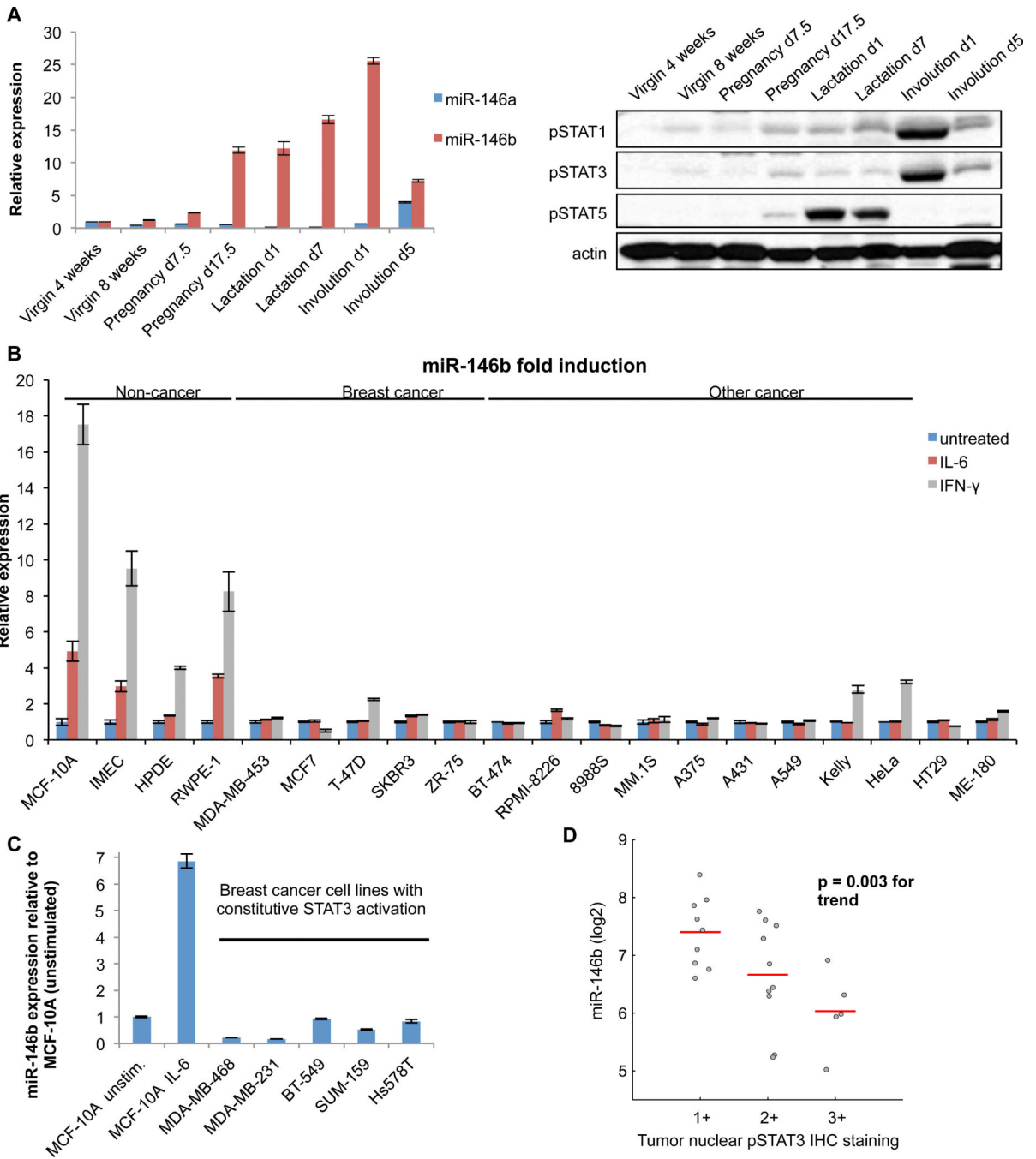
Fig. 2. STAT activation mediates miR-146b expression in normal mammary epithelium and non-transformed cells but not cancer cells

(A) Relative expression of miR-146a and –146b in mouse mammary gland tissue at indicated stages (left); immunoblots for activation of STAT1, STAT3, and STAT5 from the same samples (right) in two mice. **(B)** Cytokine induction of miR-146b in cell lines without basal STAT activation, measured 48 hours after cytokine treatment. **(C)** MiR-146b expression was measured in 5 breast cancer cell lines with constitutively-active STAT3 or in IL-6-stimulated MCF-10A cells, and normalized to U6 snRNA. Data in (B) and (C) are representative of two independent experiments **(D)** Relationship of miR-146b expression

and STAT3 phosphorylation in 24 invasive human breast tumor specimens; p=0.003 by Pearson correlation.

A

B

C

TCGA Breast Cancer Data Set (N = 524)

rho = -0.40
p = 4.7x10^{-22}

D

E

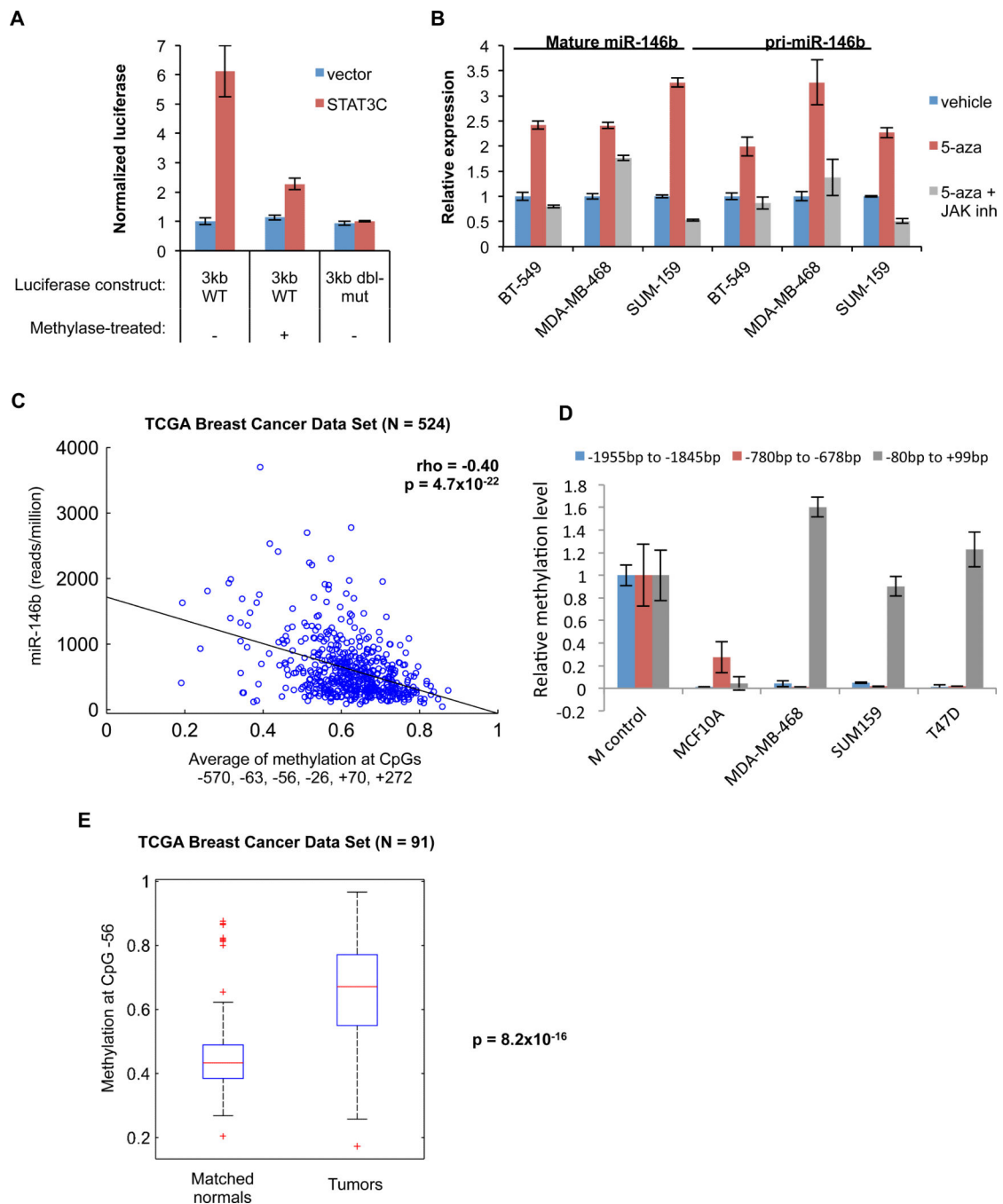TCGA Breast Cancer Data Set (N = 91)

p = 8.2x10^{-16}

Fig. 3. DNA methylation counteracts STAT3 activity at the *miR-146b* promoter and inhibits miR-146b expression in vitro and in vivo

(**A**) Luciferase activity of the indicated miR-146b reporters, with or without prior treatment by SssI methylase, was assessed in MCF-10A cells 24 hours post-transfection with STAT3C. Methylation by SssI was confirmed by protection of reporter plasmid from HpaII digestion (fig. S4A). (**B**) Expression of primary and mature miR-146b was assessed in breast cancer cells with constitutive STAT3 activation after demethylation by 5-azacytidine alone or in combination with JAK inhibitor. (**C**) Correlation of miR-146b expression (reads per

million) and *miR-146b* promoter CpG methylation in 524 breast cancer samples from TCGA. Pearson correlation and the least-squares regression line are shown. **(D)** Q-MSP assessing methylation of CpG sites −63, −56, and +70 bp relative to *miR-146b*. M control: fully methylated sequence. **(E)** *miR-146b* promoter methylation assessed in 91 TCGA breast cancer samples that have corresponding matched normal tissue (rank-sum test). In (A) and (D), data are means ± SD from two biological replicates. In (B), data representative means ± SE from one of two independent experiments.
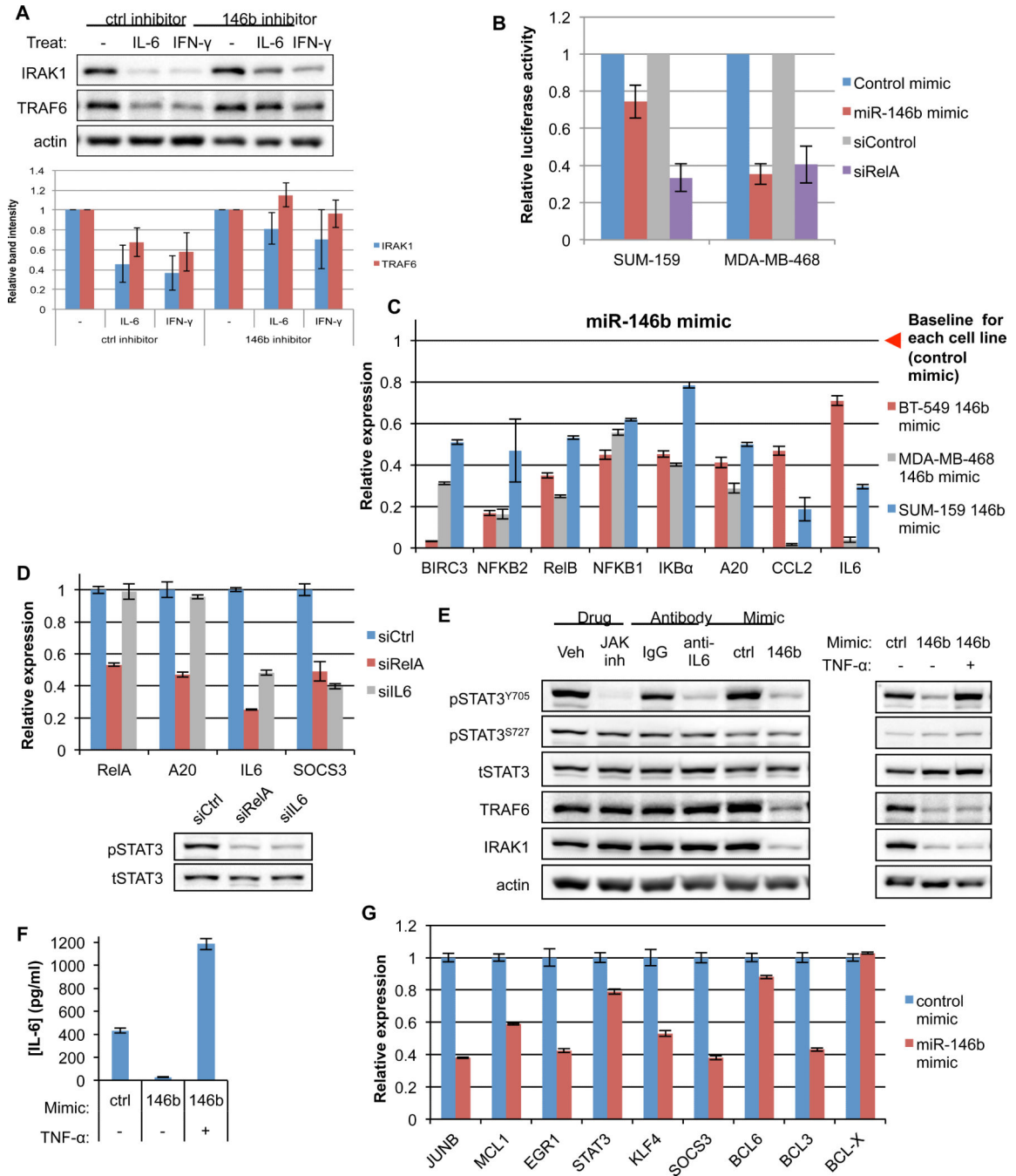
Fig. 4. miR-146b inhibits NF-κB-dependent IL-6 expression and autocrine IL-6-dependent STAT3 activation

(**A**) Western blot of MCF-10A cells transfected with control or miR-146b inhibitor, then treated with IL-6 or IFN-γ (20 ng/ml) for 72 hours to induce miR-146b. Densitometric quantitation is shown below. (**B**) NF-κB-dependent luciferase activity (relative to a *Renilla* luciferase control) in breast cancer cell lines transfected with a miR-146b mimic or control. Cells treated with RNAi to the p65 subunit of NF-κB served as a positive control. (**C**) NF-κB target gene expression in 3 breast cancer cell lines 72 hours after miR-146b mimic

transfection relative to control mimic in each respective cell line. **(D)** Gene expression and STAT3 tyrosine phosphorylation assessed in SUM-159 cells 72 hours after transfection with the indicated siRNA pools. **(E)** Immunoblot of SUM-159 cells treated with JAK inhibitor (2 hours), IL-6 neutralizing antibody (6 hours), or miR-146b mimic transfection (72 hours). Separately (right), cells transfected with miR-146b mimic were also treated with TNF-α (5 ng/ml). Data are means ± SD from two biological replicates. **(F)** ELISA measurement of IL-6 concentration (mean ± SD) in conditioned medium from SUM-159 cells. **(G)** Expression of STAT3 target genes in SUM-159 cells 72 hours after transfection with miR-146b mimic. Data are representative of at least two independent experiments. In (B), (C), and (F), qRT-PCR data are representative means ± SE from one of 2 independent experiments.
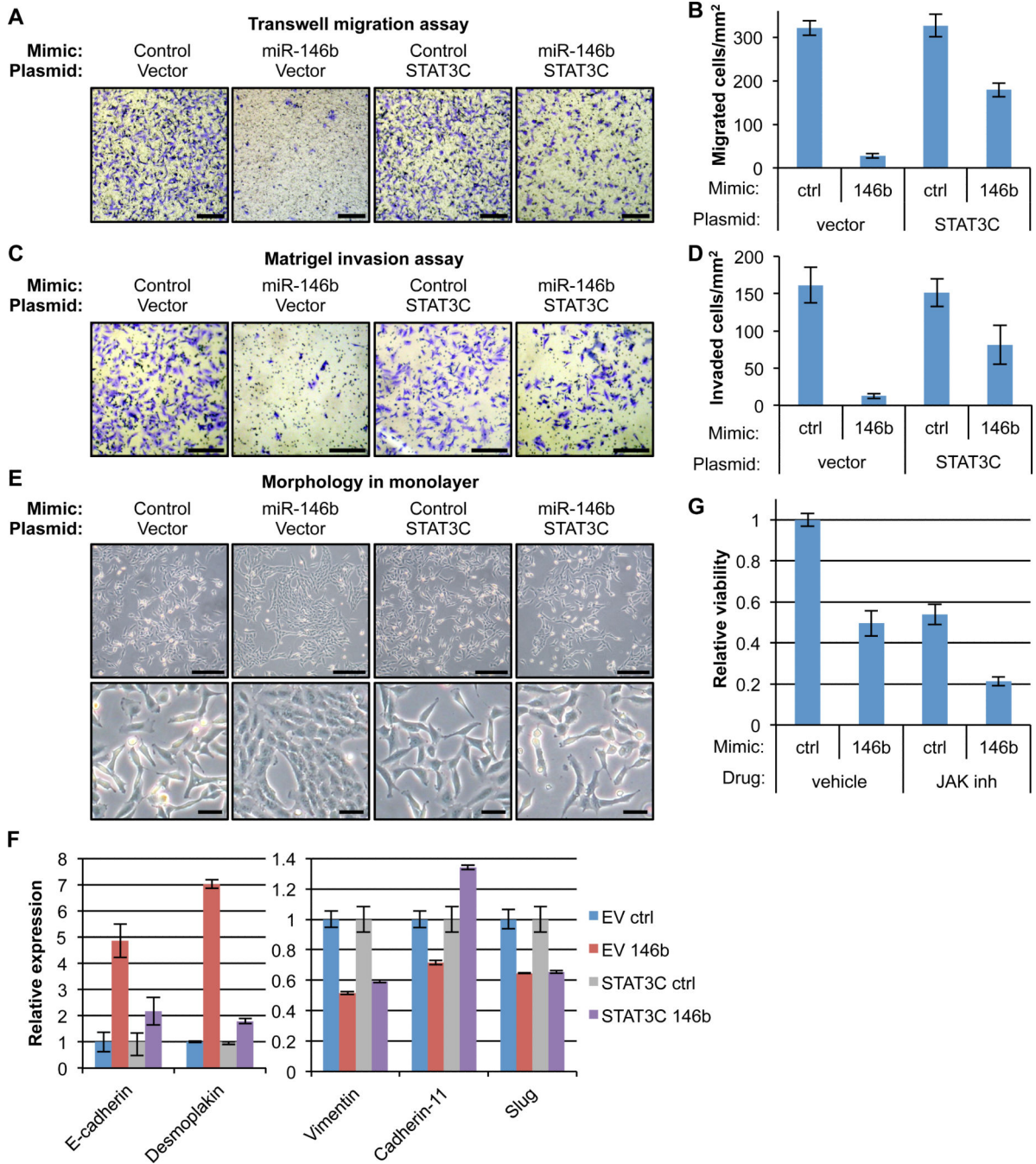
Fig. 5. MiR-146b inhibits IL-6/STAT3-driven migration, invasion, and mesenchymal phenotype of cancer cells

(A-B) Microscopy and quantitation of transwell migration assays of SUM-159 cells, transduced with either empty vector or STAT3C, after transfection with control or miR-146b mimic. Scale bar, 250μm. **(C-D)** Experiment performed as in panels A-B but using Matrigel invasion assays. **(E)** Morphological appearance of SUM-159 cells after 72 hours transfection with control or miR-146b mimic. Scale bar, 250 μm (upper) and 50 μm (lower). Data and images in (A) to (E) are means ± SD from two independent experiments. **(F)** Presence of

epithelial and mesenchymal markers in SUM-159 cells 72 hours after transfection with control or miR-146b mimic. Data are representative means ± SE from one of X independent experiments. **(G)** Viability of SUM-159 cells 96 hours after treatment with JAK inhibitor (500nM), transfection with miR-146b mimic, or both. Data are means ± SD from three biological replicates.
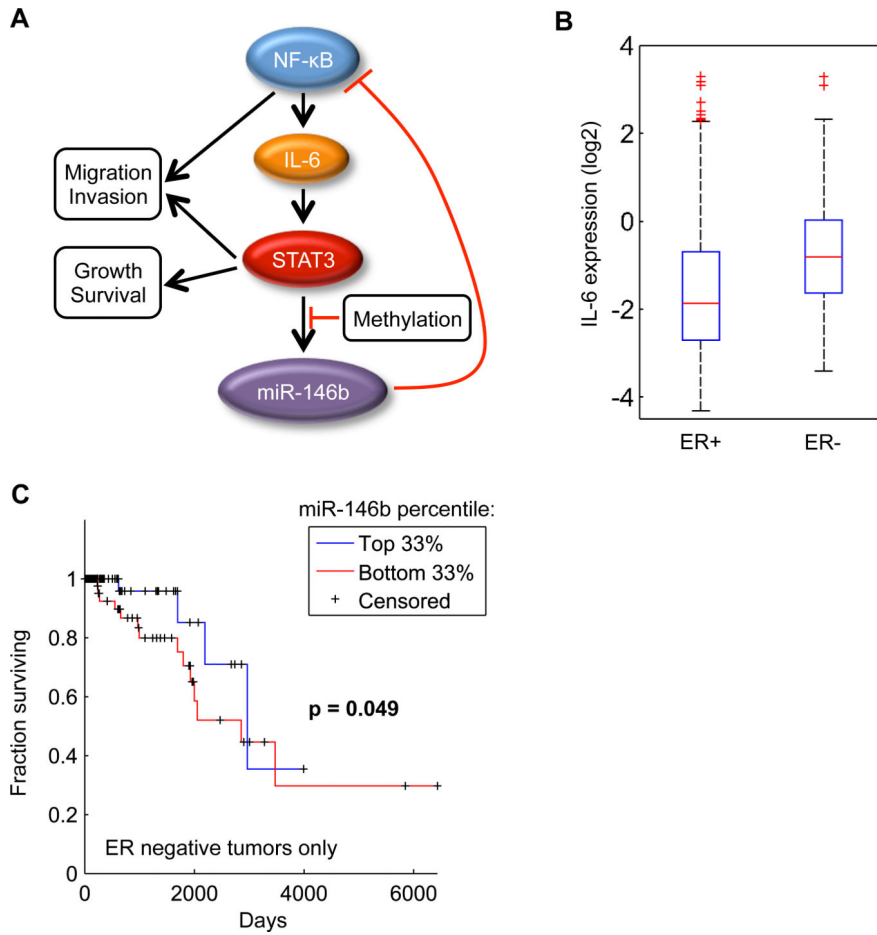
Fig. 6. Significance of STAT3 regulation of miR-146b in human breast cancers
(**A**) Schematic representation of the proposed regulatory circuit integrating STAT3, miR-146b, NF-κB, and IL-6. (**B**) *IL6* expression in TCGA breast cancer samples according to ER status ($p = 1.7 \times 10^{-7}$, rank-sum test). (**C**) Kaplan-Meier survival curves of upper tertile versus bottom tertile of miR-146b expression (read count per sample) in TCGA patients with ER-negative breast cancer (log-rank test).